

RESEARCH ARTICLE

Interpolated DFT Algorithm for Frequency Estimation by Using Maximum Sidelobe Decay Windows

HUIHAO WU¹, HUANHUA SONG, YUCHAN BAI, LEI FAN¹, JIYU JIN, AND JUN XING

School of Information Science and Engineering, Dalian Polytechnic University, Dalian 116034, China

Corresponding authors: Lei Fan (fanlei@dlpu.edu.cn) and Jiyu Jin (jinjiyu@dlpu.edu.cn)

This work was supported by the 2021 Scientific Research Projects of Liaoning Provincial Department of Education under Grant LJKZ0515, Grant LJKZ0519, and Grant LJKZ0518.

ABSTRACT A sinusoidal frequency estimator based on interpolated Discrete Fourier Transform (DFT) algorithm by using Maximum Sidelobe Decay (MSD) windows is proposed in this paper. Firstly, the received sinusoid is weighted by an appropriate MSD window. Then DFT is carried out on the weighted sinusoid and the coarse estimation is acquired by finding the position of the maximum DFT sample. Different from all the existing algorithms, the presented estimator adopts the maximum DFT sample and two Discrete Time Fourier Transform (DTFT) spectral lines which are on the same side of the maximum DFT sample in the fine estimation step. MSE formulas of the presented estimator in additive white noise are derived. Simulation results indicate that the presented estimator outperforms the competing estimators.

INDEX TERMS DFT, DTFT, frequency estimation, MSD window.

I. INTRODUCTION

Frequency estimation of sinusoid is an essential subject in the area of signal processing, and it is widely used in communications, radar signal processing, sonar, electronic measurement, power systems and so on. For instance, the oscillation frequency may deviate from the nominal frequency. And the relative movement between the receiver and transmitter is common which will lead to Doppler shift. Therefore, carrier frequency offset is common in mobile communication systems. Estimating the carrier frequency offset accurately is significant for the multicarrier communication systems.

Many researchers have presented their sinusoidal frequency estimators. The sinusoidal frequency estimators are categorized into two types: algorithms in time domain [1], [2], [3], [4], [5], [6], [7], [8] and algorithms in frequency domain [9], [10], [11], [12], [13], [14], [15], [16], [17], [18]. Algorithms in time domain include maximum likelihood estimators [1], [2], [3], auto-correlation estimators [4], [5], [6], [7], linear predictions estimators [8] and so on.

The associate editor coordinating the review of this manuscript and approving it for publication was Brian Ng¹.

Generally, the common problem of time-domain methods is that they have relatively high computational complexity and high hardware requirements. Therefore, time-domain algorithms are not suitable to be applied for some real-time applications. Algorithms in frequency domain are more efficient and usually based on DFT. The DFT-based estimators generally have two steps. Firstly, DFT is performed, and the coarse estimation is done by finding the discrete frequency index number of the maximum DFT sample. Next in the fine estimation stage, several spectrum lines near the maximum one are utilized to interpolate the signal frequency. The existing DFT-based estimators differ from each other only in the fine estimation. In [9], Aboutanios and Mulgrew employ the two DTFT spectral lines located at the midpoints between the maximum DFT sample and its two neighbors. Candan adopts the maximum DFT spectrum line and two adjacent DFT spectrum lines in the fine estimation [10]. Liao and Chen adopts phase correction of DFT coefficients which removes the phase term to reduce the estimation bias [11]. An asymptotically unbiased method is proposed which uses hybrid half-shifted and q -shifted DTFT interpolation and can converge in two iterations [12]. In [13], the maximum DFT

sample and two DTFT samples which are at any places in the DTFT main lobe are utilized to realize the fine estimation.

The above algorithms [1], [2], [3], [4], [5], [6], [7], [8], [9], [10], [11], [12], [13], [14], [15], [16], [17], [18] perform frequency estimation in white noise by using rectangular window. When interfering signals exist besides white noise, the sinusoid can be weighted by non-rectangular windows to reduce the impact of the interfering signals. In recent years, several estimators based on non-rectangular windows have been presented [17], [19], [20], [21], [22], [23], [24], [25], [26], [27], [28]. Based on the estimator in [10], Candan proposes to estimate the frequency by using an arbitrary non-rectangular window [19]. In [20], a generalization of the algorithm in [9] is presented (called IpDTFT-NR algorithm). It is based on MSD windows and suppresses the noise maximally for frequency estimator by DTFT interpolation. In [21], Belega generalizes the methods in [9] and [10] to the situation when the received sinusoid is multiplied with MSD windows. The PSF-IpDFTc and the HPSF-IpDFTc algorithms based on Hanning window are presented to estimate the frequency of noisy and noisy harmonically distorted sinusoidal signals, respectively [22]. The Parabolic Interpolated DTFT (PIpDTFT) algorithm is extended to the case when the signal is weighted by MSD windows and the frequency estimation accuracy is analyzed [27].

In this article, a sinusoidal frequency estimation algorithm based on interpolated DFT by using MSD windows is presented. Firstly, the received sinusoid is multiplied with an appropriate MSD window. Then DFT is carried out on the weighted sinusoid. And the position of the maximum DFT sample is found to acquire the coarse estimation. In the fine estimation step, the maximum DFT sample and two DTFT spectral lines which are on the same side of the maximum DFT sample are adopted. MSE formulas of the presented estimator in additive white noise are derived. Simulation experiments are carried out, and the results indicate the performance of the presented algorithm is better than that of the competing estimators.

The remaining parts of the article are arranged as follows. In Section II the presented estimation algorithm based on MSD windows is given and the MSE formulas in additive white noise are derived. Section III contrasts the present algorithm with the competing algorithms and the Cramer-Rao lower bound (CRLB). At last, Section IV draws the conclusion of the article.

II. PROPOSED ESTIMATOR AND MSE

A. PROPOSED ESTIMATOR

In this part, a frequency estimation algorithm of sinusoid based on MSD windows is presented. The sinusoidal signal is [11]

$$\begin{aligned} x[n] &= s[n] + z[n] \\ &= Ae^{j(2\pi f_0 n/f_s + \theta_0)} + z[n], n = 0, 1, \dots, N-1 \end{aligned} \quad (1)$$

where $s[n]$ is the received sinusoid to be estimated. $z[n]$ is additive white noise, with variance σ^2 and mean value zero.

f_s is the frequency of sampling, and N is the number of samples. A , f_0 and θ_0 denote the amplitude, frequency and initial phase of the sinusoid respectively.

In a noiseless case, we perform N -point DFT of the sinusoid $s[n]$, and have [14]

$$\begin{aligned} S[m+k] &= \sum_{n=0}^{N-1} Ae^{j(2\pi f_0 n/f_s + \theta_0)} e^{-j2\pi nk/N} \\ &= e^{j\theta_0} e^{j\pi \frac{N-1}{N}(\delta-k)} \frac{A \sin[\pi(\delta-k)]}{\sin[\pi(\delta-k)/N]}, \\ & \quad k = 0, 1, \dots, N-1 \end{aligned} \quad (2)$$

where m is the discrete frequency index value of the maximum DFT sample. δ represents the relative frequency deviation between the maximum DFT sample and the signal frequency, $\delta \in (-0.5, 0.5)$. $\Delta f = f_s/N$ is the frequency interval between two adjacent DFT samples. We can express the sinusoidal frequency as $f_0 = (m + \delta)\Delta f$. At the coarse stage, we need to search the position of the maximum DFT sample $S[m]$. For the convenience of expression, $S[m+k]$ is denoted as S_k . Then the expression of the maximum DFT sample is

$$S[m] = S_0 = e^{j[\theta_0 + \pi\delta(1-1/N)]} \frac{A \sin(\pi\delta)}{\sin(\pi\delta/N)} \quad (3)$$

In the next step, the fine estimation of f_0 is actually to estimate the relative frequency deviation δ . We use the maximum DFT sample S_0 and two DTFT samples $S_{0.1}$ and $S_{0.2}$ (or $S_{-0.1}$ and $S_{-0.2}$) to obtain the fine estimate. The DTFT sample value at the location $f = (m+q)\Delta f$ is written as

$$S_q = e^{j[\theta_0 - \pi(q-\delta)(1-1/N)]} \frac{A \sin(\pi(q-\delta))}{\sin(\pi(q-\delta)/N)} \quad (4)$$

Substituting $q = 0.1$ and 0.2 into the above formula respectively, the expressions of the two DTFT spectrum lines $S_{0.1}$ and $S_{0.2}$ can be written as

$$S_{0.1} = e^{j[\theta_0 - \pi(0.1-\delta)(1-1/N)]} \frac{A \sin(\pi(0.1-\delta))}{\sin(\pi(0.1-\delta)/N)} \quad (5)$$

$$S_{0.2} = e^{j[\theta_0 - \pi(0.2-\delta)(1-1/N)]} \frac{A \sin(\pi(0.2-\delta))}{\sin(\pi(0.2-\delta)/N)} \quad (6)$$

Then the absolute values of S_0 , $S_{0.1}$ and $S_{0.2}$ are utilized to deduce the estimation formula of δ . After some derivation, we get

$$\frac{|S_{0.1}|}{|S_0|} = \frac{\sin(0.1\pi) \cot(\pi\delta) - \cos(0.1\pi)}{\sin(0.1\pi/N) \cot(\pi\delta/N) - \cos(0.1\pi/N)} \quad (7)$$

$$\frac{|S_{0.2}|}{|S_0|} = \frac{\sin(0.2\pi) \cot(\pi\delta) - \cos(0.2\pi)}{\sin(0.2\pi/N) \cot(\pi\delta/N) - \cos(0.2\pi/N)} \quad (8)$$

From (7) and (8), we have derived in (9), as shown at the bottom of the next page.

The estimation expression of δ is written in (10), as shown at the bottom of the next page.

When using the two DTFT samples $S_{-0.1}$ and $S_{-0.2}$ located on the left of the maximum DFT sample, after similar derivation, we can obtain in (11), as shown at the bottom of the next page.

In a more general case, we can use the spectral lines $S_0, S_{i/2}$ and S_i to estimate the frequency (the variable $i \in [-1, 1]$). After similar derivation as above, we have derived in (12), as shown at the bottom of the page.

The frequency estimation RMSEs of the above estimator versus $|i|$ are shown in Fig. 1 for $N = 16$ and $SNR = 20\text{dB}$. $|i|$ varies from 0.02 to 1 with a step of 0.02. The RMSEs are normalized to the square root of the CRLB (RCRLB). When the frequency, amplitude and initial phase of a complex sinusoidal signal are unknown, the CRLB can be written as [1]

$$\text{CRLB} = \min \text{var}(\hat{f}) = \frac{3f_s^2}{2\pi^2 N(N^2 - 1) \cdot \text{SNR}} \quad (13)$$

It can be seen that when $|\delta| = 0.05$ and $|i| \leq 0.2$, RMSEs of the proposed estimator are very close to the RCRLB. Therefore, we can perform the preliminary fine estimation of δ with a certain method firstly. Then with the value of the preliminary estimate, we can determine which of the estimation formula ((10) or (11)) should be used and the complex values of the three spectral lines used by the final fine estimation can be renewed. The residual value of $|\delta|$ in the final fine estimation will be very small. This situation is very similar to the results shown by the RMSEs curve for $|\delta| = 0.05$ in Fig. 1. When $|\delta| = 0.05$, the performance for $|i| \leq 0.2$ is almost unchanged and is much better than the performance for $|i| > 0.2$. Therefore, we choose $|i| = 0.2$ in our method.

Next, we extend the above rectangular windowing estimation algorithm to the case of MSD windowing. The MSD window is also known as the Rife-Vincent class I window, belonging to the $\sin^\alpha(x)$ window for $\alpha = 0, 2, 4, \dots$ [26]. Among all H -term cosine windows, the sidelobe decay rate of MSD window is $6(2H - 1)$ dB/octave which is highest [23].

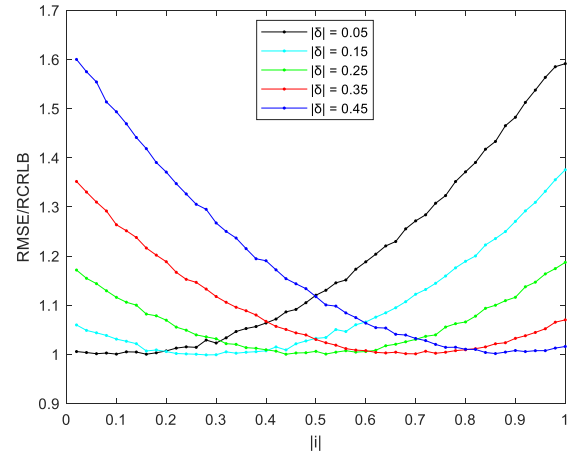


FIGURE 1. RMSEs of proposed estimator versus $|i|$ ($N = 16, SNR = 20\text{dB}$).

The expression of H -term MSD window is expressed as [21]

$$w[n] = \sum_{h=0}^{H-1} (-1)^h a_h \cos\left(2\pi \frac{h}{N} n\right), n = 0, 1, \dots, N - 1 \quad (14)$$

in which $H \geq 1$. a_h denotes the coefficient of the window and can be expressed as [23]

$$a_0 = \frac{C^{H-1}}{2^{2H-2}}, a_h = \frac{C^{H-h-1}}{2^{2H-3}}, h = 1, 2, \dots, H - 1 \quad (15)$$

in which $C_g^l = g! / [(g-l)!l!]$. It is worth noticing that for $H = 1$ the MSD window is actually the rectangular window.

The sampled sinusoid multiplied by an appropriate MSD window can be written as

$$s_w[n] = s[n] \cdot w[n], n = 0, 1, \dots, N - 1 \quad (16)$$

$$\cot\left(\frac{\pi \delta}{N}\right) = \frac{|S_0| \sin(0.1\pi) + |S_{0.2}| \cos\left(\frac{0.2\pi}{N}\right) \sin(0.1\pi) - |S_{0.1}| \cos\left(\frac{0.1\pi}{N}\right) \sin(0.2\pi)}{|S_{0.2}| \sin\left(\frac{0.2\pi}{N}\right) \sin(0.1\pi) - |S_{0.1}| \sin\left(\frac{0.1\pi}{N}\right) \sin(0.2\pi)} \quad (9)$$

$$\hat{\delta} = \frac{N}{\pi} \tan^{-1} \left[\frac{|S_{0.2}| \sin\left(\frac{0.2\pi}{N}\right) - 2|S_{0.1}| \sin\left(\frac{0.1\pi}{N}\right) \cos(0.1\pi)}{|S_0| + |S_{0.2}| \cos\left(\frac{0.2\pi}{N}\right) - 2|S_{0.1}| \cos\left(\frac{0.1\pi}{N}\right) \cos(0.1\pi)} \right] \quad (10)$$

$$\hat{\delta} = \frac{N}{\pi} \tan^{-1} \left[\frac{|S_{-0.2}| \sin\left(\frac{0.2\pi}{N}\right) - 2|S_{-0.1}| \sin\left(\frac{0.1\pi}{N}\right) \cos(0.1\pi)}{-|S_0| - |S_{-0.2}| \cos\left(\frac{0.2\pi}{N}\right) + 2|S_{-0.1}| \cos\left(\frac{0.1\pi}{N}\right) \cos(0.1\pi)} \right] \quad (11)$$

$$\hat{\delta} = \frac{N}{\pi} \tan^{-1} \left\{ \frac{|S_i| \sin\left(\frac{\pi i}{N}\right) - 2|S_{i/2}| \sin\left(\frac{\pi i}{2N}\right) \cos\left(\frac{\pi i}{2}\right)}{|S_0| + |S_i| \cos\left(\frac{\pi i}{N}\right) - 2|S_{i/2}| \cos\left(\frac{\pi i}{2N}\right) \cos\left(\frac{\pi i}{2}\right)} \right\} \quad (12)$$

The DTFT of $s_w[n]$ is

$$S_w(\lambda) = AW(\lambda - \nu) e^{j\theta_0} \quad (17)$$

where $W(\cdot)$ is the DTFT of the window function $w[n]$. And $\nu = m + \delta$ is the number of observed signal cycles. If it is assumed that N is much larger than 1, then the DTFT of $w[n]$ is [21]

$$\begin{aligned} W(\lambda) &= \frac{N \sin(\pi\lambda)}{\pi} \sum_{h=0}^{H-1} (-1)^h a_h \frac{\lambda}{\lambda^2 - h^2} e^{-j\pi\lambda} \\ &= \tilde{W}(\lambda) e^{-j\pi\lambda}, n = 0, 1, \dots, N - 1 \end{aligned} \quad (18)$$

where

$$\tilde{W}(\lambda) = \frac{N \sin(\pi\lambda)}{\pi} \sum_{h=0}^{H-1} (-1)^h a_h \frac{\lambda}{\lambda^2 - h^2} \quad (19)$$

Calculating the derivative of $\tilde{W}(\lambda)$, we can get

$$\begin{aligned} \tilde{W}'(\lambda) &= \frac{N}{\pi} [\sin(\pi\lambda) + \pi\lambda \cos(\pi\lambda)] \sum_{h=0}^{H-1} \frac{(-1)^h a_h}{\lambda^2 - h^2} \\ &\quad - \frac{2N}{\pi} \lambda^2 \sin(\pi\lambda) \sum_{h=0}^{H-1} \frac{(-1)^h a_h}{(\lambda^2 - h^2)^2} \end{aligned} \quad (20)$$

Then we replace the spectral lines in the square brackets of (10) with the corresponding DTFT spectral lines of the weighted sinusoid. And we obtain in (21), as shown at the bottom of the next page, where $S_w(m)$ is the maximum DFT sample of $s_w[n]$, $S_w(m + 0.1)$ and $S_w(m + 0.2)$ are two DTFT samples which are located at $f = (m + 0.1)\Delta f$ and $f = (m + 0.2)\Delta f$. According to (17), (18) and (19), let $\lambda = m, m + 0.1$ and $m + 0.2$, we have

$$|S_w(m)| = |A| \tilde{W}(-\delta) \quad (22)$$

$$|S_w(m + 0.1)| = |A| \tilde{W}(0.1 - \delta) \quad (23)$$

$$|S_w(m + 0.2)| = |A| \tilde{W}(0.2 - \delta) \quad (24)$$

According to (21)-(24), we get in (25), as shown at the bottom of the next page.

Then the first-order Taylor series expansions are performed for $\tilde{W}(-\delta)$, $\tilde{W}(0.1 - \delta)$ and $\tilde{W}(0.2 - \delta)$ near 0, 0.1 and 0.2 respectively. And we ignore the higher order terms, then we have

$$\tilde{W}(-\delta) \approx \tilde{W}(0) - \tilde{W}'(0) \delta \quad (26)$$

$$\tilde{W}(0.1 - \delta) \approx \tilde{W}(0.1) - \tilde{W}'(0.1) \delta \quad (27)$$

$$\tilde{W}(0.2 - \delta) \approx \tilde{W}(0.2) - \tilde{W}'(0.2) \delta \quad (28)$$

Substituting (26)-(28) into (25), we have derived in (29), as shown at the bottom of the next page.

According to [21], $\tilde{W}'(0) = 0$. After some algebra, the following formula can be obtained in (30), as shown at the bottom of the next page.

Then we set

$$B = \tilde{W}(0.2) \sin\left(\frac{0.2\pi}{N}\right)$$

TABLE 1. Steps of the presented estimator.

Step	Description
1	Multiply the sinusoid with an appropriate MSD window and get $x_w[n] = x[n] \cdot w[n], n = 0, 1, K, N - 1$
2	Carry out N -point DFT of $x_w[n]$, and find m
3	Using the estimator in [23] ($i=1$), $\hat{\delta}_{w1}$ is obtained
4	Compute the difference between $ \hat{\delta}_{w1} $ and 0.1, getting $p = \hat{\delta}_{w1} - 0.1$
5	If $\hat{\delta}_{w1} > 0$, compute $X_w(m+p)$, $X_w(m+p+0.1)$ and $X_w(m+p+0.2)$ via $X_w(m+Q_1) = \sum_{n=0}^{N-1} x_w[n] e^{-j2\pi n \frac{m+Q_1}{N}}$, $Q_1 = p, p+0.1, p+0.2$, and obtain $\hat{\delta}_w$ via (35) and (21). The final estimate is $\hat{\delta}_f = \hat{\delta}_{w1} - 0.1 + \hat{\delta}_w$ ($\hat{f} = (m + \hat{\delta}_{w1} - 0.1 + \hat{\delta}_w)\Delta f$)
6	If $\hat{\delta}_{w1} \leq 0$, compute $X_w(m-p)$, $X_w(m-p-0.1)$ and $X_w(m-p-0.2)$ via $X_w(m+Q_2) = \sum_{n=0}^{N-1} x_w[n] e^{-j2\pi n \frac{m+Q_2}{N}}$, $Q_2 = -p, -p-0.1, -p-0.2$ and get $\hat{\delta}_w$ via (36) and (37). The final estimate is $\hat{\delta}_f = \hat{\delta}_{w1} + 0.1 + \hat{\delta}_w$ ($\hat{f} = (m + \hat{\delta}_{w1} + 0.1 + \hat{\delta}_w)\Delta f$)

$$-2\tilde{W}(0.1) \sin\left(\frac{0.1\pi}{N}\right) \cos(0.1\pi) \quad (31)$$

$$C = \tilde{W}'(0.2) \sin\left(\frac{0.2\pi}{N}\right) - 2\tilde{W}'(0.1) \sin\left(\frac{0.1\pi}{N}\right) \cos(0.1\pi) \quad (32)$$

$$D = \tilde{W}(0) + \tilde{W}(0.2) \cos\left(\frac{0.2\pi}{N}\right) - 2\tilde{W}(0.1) \cos\left(\frac{0.1\pi}{N}\right) \cos(0.1\pi) \quad (33)$$

$$E = \tilde{W}'(0.2) \cos\left(\frac{0.2\pi}{N}\right) - 2\tilde{W}'(0.1) \cos\left(\frac{0.1\pi}{N}\right) \cos(0.1\pi) \quad (34)$$

From (30)-(34), the estimation expression for δ is

$$\hat{\delta} = \frac{YD - B}{YE - C} \quad (35)$$

When the maximum DFT sample $S_w(m)$ and the two DTFT samples $S_w(m - 0.1)$ and $S_w(m - 0.2)$ are used, after similar derivation, we can obtain

$$\hat{\delta} = -\frac{VD + B}{VE + C} \quad (36)$$

where (37), as shown at the bottom of the next page.

The steps of the presented estimator are listed in Table. 1. In the process of estimating the frequency with the algorithm in this paper, it is necessary to preliminarily determine which of the estimation formula (35) or (36) should be used for the fine estimation. Therefore, we use the estimator in [23] ($i = 1$) to acquire a preliminary estimation value $\hat{\delta}_{w1}$ of the relative frequency deviation. Firstly, we multiply the sinusoid with an appropriate MSD window. Then, we perform DFT on the weighted sinusoid, and find the position of the maximum DFT sample to obtain a coarse estimate. With the value of $\hat{\delta}_{w1}$, the complex values of the three samples used by the presented algorithm are renewed. Finally, the fine estimation is obtained via (35) and (21) when $\hat{\delta}_{w1} > 0$ or via (36) and (37) when $\hat{\delta}_{w1} \leq 0$.

B. MSE OF $\hat{\delta}$

In this part, the MSE of $\hat{\delta}$ via (35) and (21) (or (36) and (37)) in the background of additive white noise is analyzed. The signal model can be written as

$$x_w[n] = s_w[n] + z_w[n], n = 0, 1, \dots, N - 1 \quad (38)$$

in which $z_w[n] = z[n] \cdot w[n]$.

We perform N -point DFT of $x_w[n]$ and can get

$$X_w[k] = S_w[k] + Z_w[k], k = 0, 1, \dots, N - 1 \quad (39)$$

According to the Appendix, the MSE formulas of the proposed estimator can be obtained. When $\delta \neq 0.2, 0.1$ and 0 ,

the MSE formula of $\hat{\delta}$ via (35) and (21) is derived in (40), as shown at the bottom of the next page.

When $\delta = 0.2$, we use $\lim_{x \rightarrow 0} [\sin(x)/x] = 1$ for the calculation of $\tilde{W}(0.2 - \delta)$ in (40). Then we derived in (41), as shown at the bottom of the next page.

When $\delta = 0.1$, $\lim_{x \rightarrow 0} [\sin(x)/x] = 1$ is used for the calculation of $\tilde{W}(0.1 - \delta)$ in (40). Then we derived in (42), as shown at the bottom of the next page.

When $\delta = 0$, we utilize $\lim_{x \rightarrow 0} [\sin(x)/x] = 1$ for the calculation of $\tilde{W}(\delta)$ in (40). Then we obtain in (43), as shown at the bottom of the next page.

When $\delta \neq -0.2, -0.1$ and 0 , the MSE formula of $\hat{\delta}$ via (36) and (37) is derived in (44), as shown at the bottom of page.

When $\delta = -0.2$, the MSE formula of $\hat{\delta}$ via (36) and (37) is the same as (41). When $\delta = -0.1$, the MSE formula of $\hat{\delta}$ is the same as (42) and when $\delta = 0$, the MSE formula is the same as (43).

When $N = 16$ and $SNR = 10$ dB, the analytical RMSE is illustrated in Fig. 2. Fig. 2 shows that the analytical RMSE reaches its minimum around at $|\delta| = 0.05$. The minimum values of RMSE/RCRLB for two-term MSD windowing method and three-term MSD windowing method are approximately 1.5455 and 2.1555 respectively. The minimum values of the analytical RMSE of the proposed method via (40)-(43) are the same as those values via (41)-(44).

The MSE of $\hat{\delta}_{w1}$ in the third step of Table. 1 is [23]

$$Y = \frac{|S_w(m + 0.2)| \sin\left(\frac{0.2\pi}{N}\right) - 2 |S_w(m + 0.1)| \sin\left(\frac{0.1\pi}{N}\right) \cos(0.1\pi)}{|S_w(m)| + |S_w(m + 0.2)| \cos\left(\frac{0.2\pi}{N}\right) - 2 |S_w(m + 0.1)| \cos\left(\frac{0.1\pi}{N}\right) \cos(0.1\pi)} \quad (21)$$

$$Y = \frac{\tilde{W}(0.2 - \delta) \sin\left(\frac{0.2\pi}{N}\right) - 2\tilde{W}(0.1 - \delta) \sin\left(\frac{0.1\pi}{N}\right) \cos(0.1\pi)}{\tilde{W}(-\delta) + \tilde{W}(0.2 - \delta) \cos\left(\frac{0.2\pi}{N}\right) - 2\tilde{W}(0.1 - \delta) \cos\left(\frac{0.1\pi}{N}\right) \cos(0.1\pi)} \quad (25)$$

$$Y = \frac{[\tilde{W}(0.2) - \tilde{W}'(0.2)\delta] \sin\left(\frac{0.2\pi}{N}\right) - 2[\tilde{W}(0.1) - \tilde{W}'(0.1)\delta] \sin\left(\frac{0.1\pi}{N}\right) \cos(0.1\pi)}{[\tilde{W}(0) - \tilde{W}'(0)\delta] + [\tilde{W}(0.2) - \tilde{W}'(0.2)\delta] \cos\left(\frac{0.2\pi}{N}\right) - 2[\tilde{W}(0.1) - \tilde{W}'(0.1)\delta] \cos\left(\frac{0.1\pi}{N}\right) \cos(0.1\pi)} \quad (29)$$

$$Y = \frac{[\tilde{W}(0.2) \sin\left(\frac{0.2\pi}{N}\right) - 2\tilde{W}(0.1) \sin\left(\frac{0.1\pi}{N}\right) \cos(0.1\pi)] - \delta [\tilde{W}'(0.2) \sin\left(\frac{0.2\pi}{N}\right) - 2\tilde{W}'(0.1) \sin\left(\frac{0.1\pi}{N}\right) \cos(0.1\pi)]}{[\tilde{W}(0) + \tilde{W}(0.2) \cos\left(\frac{0.2\pi}{N}\right) - 2\tilde{W}(0.1) \cos\left(\frac{0.1\pi}{N}\right) \cos(0.1\pi)] - \delta [\tilde{W}'(0.2) \cos\left(\frac{0.2\pi}{N}\right) - 2\tilde{W}'(0.1) \cos\left(\frac{0.1\pi}{N}\right) \cos(0.1\pi)]} \quad (30)$$

$$V = \frac{|S_w(m - 0.2)| \sin\left(\frac{0.2\pi}{N}\right) - 2 |S_w(m - 0.1)| \sin\left(\frac{0.1\pi}{N}\right) \cos(0.1\pi)}{-|S_w(m)| - |S_w(m - 0.2)| \cos\left(\frac{0.2\pi}{N}\right) + 2 |S_w(m - 0.1)| \cos\left(\frac{0.1\pi}{N}\right) \cos(0.1\pi)} \quad (37)$$

The MSE of the final estimate $\hat{\delta}_f$ in the fifth or sixth step of Table. 1 will be very close to the minimum value of (40) or (44). This can be seen in the simulation results of Fig. 5 in the next section.

III. SIMULATION RESULTS

In this part, simulation experiments are conducted, and the performance of the presented estimation algorithm is compared with the competing algorithms. The algorithms

$$\begin{aligned}
 & E \left[(\hat{\delta} - \delta)^2 \right] \\
 & \approx \frac{\left\{ |W_2(0)| \left[\left(\frac{0.2\pi}{N} D - B \right) - \delta \left(\frac{0.2\pi}{N} E - C \right) \right]^2 + 4 |W_2(0)| \cos^2(0.1\pi) \left[\left(\frac{0.1\pi}{N} D - B \right) - \delta \left(\frac{0.1\pi}{N} E - C \right) \right]^2 + |W_2(0)| (B - \delta C)^2 \right\}}{2 \cdot SNR \cdot \left\{ \tilde{W}(0.2 - \delta) \left(\frac{0.2\pi}{N} E - C \right) - 2\tilde{W}(0.1 - \delta) \cos(0.1\pi) \left(\frac{0.1\pi}{N} E - C \right) - \tilde{W}(\delta) C \right\}^2} \\
 & + \frac{\left\{ 4 |W_2(0.1\Delta f)| \cos(0.1\pi) \left[\left(\frac{0.1\pi}{N} D - B \right) - \delta \left(\frac{0.1\pi}{N} E - C \right) \right] (B - \delta C) - 2 |W_2(0.2\Delta f)| \left[\left(\frac{0.2\pi}{N} D - B \right) - \delta \left(\frac{0.2\pi}{N} E - C \right) \right] (B - \delta C) \right\}}{2 \cdot SNR \cdot \left\{ \tilde{W}(0.2 - \delta) \left(\frac{0.2\pi}{N} E - C \right) - 2\tilde{W}(0.1 - \delta) \cos(0.1\pi) \left(\frac{0.1\pi}{N} E - C \right) - \tilde{W}(\delta) C \right\}^2} \\
 & - \frac{\left\{ 4 |W_2(0.1\Delta f)| \cos(0.1\pi) \left[\left(\frac{0.2\pi}{N} D - B \right) - \delta \left(\frac{0.2\pi}{N} E - C \right) \right] \left[\left(\frac{0.1\pi}{N} D - B \right) - \delta \left(\frac{0.1\pi}{N} E - C \right) \right] \right\}}{2 \cdot SNR \cdot \left\{ \tilde{W}(0.2 - \delta) \left(\frac{0.2\pi}{N} E - C \right) - 2\tilde{W}(0.1 - \delta) \cos(0.1\pi) \left(\frac{0.1\pi}{N} E - C \right) - \tilde{W}(\delta) C \right\}^2} \tag{40}
 \end{aligned}$$

$$\begin{aligned}
 & E \left[(\hat{\delta} - \delta)^2 \right] \\
 & \approx \frac{\left\{ |W_2(0)| \left[\left(\frac{0.2\pi}{N} D - B \right) - 0.2 \left(\frac{0.2\pi}{N} E - C \right) \right]^2 + 4 |W_2(0)| \cos^2(0.1\pi) \left[\left(\frac{0.1\pi}{N} D - B \right) - 0.2 \left(\frac{0.1\pi}{N} E - C \right) \right]^2 + |W_2(0)| (B - 0.2C)^2 \right\}}{2 \cdot SNR \cdot \left\{ 0.5\pi \left(\frac{0.2\pi}{N} E - C \right) - 2\tilde{W}(0.1) \cos(0.1\pi) \left(\frac{0.1\pi}{N} E - C \right) - \tilde{W}(0.2) C \right\}^2} \\
 & + \frac{\left\{ 4 |W_2(0.1\Delta f)| \cos(0.1\pi) \left[\left(\frac{0.1\pi}{N} D - B \right) - 0.2 \left(\frac{0.1\pi}{N} E - C \right) \right] (B - 0.2C) - 2 |W_2(0.2\Delta f)| \left[\left(\frac{0.2\pi}{N} D - B \right) - 0.2 \left(\frac{0.2\pi}{N} E - C \right) \right] (B - 0.2C) \right\}}{2 \cdot SNR \cdot \left\{ 0.5\pi \left(\frac{0.2\pi}{N} E - C \right) - 2\tilde{W}(0.1) \cos(0.1\pi) \left(\frac{0.1\pi}{N} E - C \right) - \tilde{W}(0.2) C \right\}^2} \\
 & - \frac{\left\{ 4 |W_2(0.1\Delta f)| \cos(0.1\pi) \left[\left(\frac{0.2\pi}{N} D - B \right) - 0.2 \left(\frac{0.2\pi}{N} E - C \right) \right] \left[\left(\frac{0.1\pi}{N} D - B \right) - 0.2 \left(\frac{0.1\pi}{N} E - C \right) \right] \right\}}{2 \cdot SNR \cdot \left\{ 0.5\pi \left(\frac{0.2\pi}{N} E - C \right) - 2\tilde{W}(0.1) \cos(0.1\pi) \left(\frac{0.1\pi}{N} E - C \right) - \tilde{W}(0.2) C \right\}^2} \tag{41}
 \end{aligned}$$

$$\begin{aligned}
 & E \left[(\hat{\delta} - \delta)^2 \right] \\
 & \approx \frac{\left\{ |W_2(0)| \left[\left(\frac{0.2\pi}{N} D - B \right) - 0.1 \left(\frac{0.2\pi}{N} E - C \right) \right]^2 + 4 |W_2(0)| \cos^2(0.1\pi) \left[\left(\frac{0.1\pi}{N} D - B \right) - 0.1 \left(\frac{0.1\pi}{N} E - C \right) \right]^2 + |W_2(0)| (B - 0.1C)^2 \right\}}{2 \cdot SNR \cdot \left\{ \tilde{W}(0.1) \left(\frac{0.2\pi}{N} E - 2C \right) - \pi \cos(0.1\pi) \left(\frac{0.1\pi}{N} E - C \right) \right\}^2} \\
 & + \frac{\left\{ 4 |W_2(0.1\Delta f)| \cos(0.1\pi) \left[\left(\frac{0.1\pi}{N} D - B \right) - 0.1 \left(\frac{0.1\pi}{N} E - C \right) \right] (B - 0.1C) - 2 |W_2(0.2\Delta f)| \left[\left(\frac{0.2\pi}{N} D - B \right) - 0.1 \left(\frac{0.2\pi}{N} E - C \right) \right] (B - 0.1C) \right\}}{2 \cdot SNR \cdot \left\{ \tilde{W}(0.1) \left(\frac{0.2\pi}{N} E - 2C \right) - \pi \cos(0.1\pi) \left(\frac{0.1\pi}{N} E - C \right) \right\}^2} \\
 & - \frac{\left\{ 4 |W_2(0.1\Delta f)| \cos(0.1\pi) \left[\left(\frac{0.2\pi}{N} D - B \right) - 0.1 \left(\frac{0.2\pi}{N} E - C \right) \right] \left[\left(\frac{0.1\pi}{N} D - B \right) - 0.1 \left(\frac{0.1\pi}{N} E - C \right) \right] \right\}}{2 \cdot SNR \cdot \left\{ \tilde{W}(0.1) \left(\frac{0.2\pi}{N} E - 2C \right) - \pi \cos(0.1\pi) \left(\frac{0.1\pi}{N} E - C \right) \right\}^2} \tag{42}
 \end{aligned}$$

$$\begin{aligned}
 & E \left[(\hat{\delta} - \delta)^2 \right] \\
 & \approx \frac{\left\{ |W_2(0)| \left(\frac{0.2\pi}{N} D - B \right)^2 + 4 |W_2(0)| \cos^2(0.1\pi) \left(\frac{0.1\pi}{N} D - B \right)^2 + |W_2(0)| B^2 - 2 |W_2(0.2\Delta f)| \left(\frac{0.2\pi}{N} D - B \right) B \right\}}{2 \cdot SNR \cdot \left\{ \tilde{W}(0.2) \left(\frac{0.2\pi}{N} E - C \right) - 2\tilde{W}(0.1) \cos(0.1\pi) \left(\frac{0.1\pi}{N} E - C \right) - 0.5\pi C \right\}^2} \\
 & + \frac{\left\{ 4 |W_2(0.1\Delta f)| \cos(0.1\pi) \left(\frac{0.1\pi}{N} D - B \right) B - 4 |W_2(0.1\Delta f)| \cos(0.1\pi) \left(\frac{0.2\pi}{N} D - B \right) \left(\frac{0.1\pi}{N} D - B \right) \right\}}{2 \cdot SNR \cdot \left\{ \tilde{W}(0.2) \left(\frac{0.2\pi}{N} E - C \right) - 2\tilde{W}(0.1) \cos(0.1\pi) \left(\frac{0.1\pi}{N} E - C \right) - 0.5\pi C \right\}^2} \tag{43}
 \end{aligned}$$

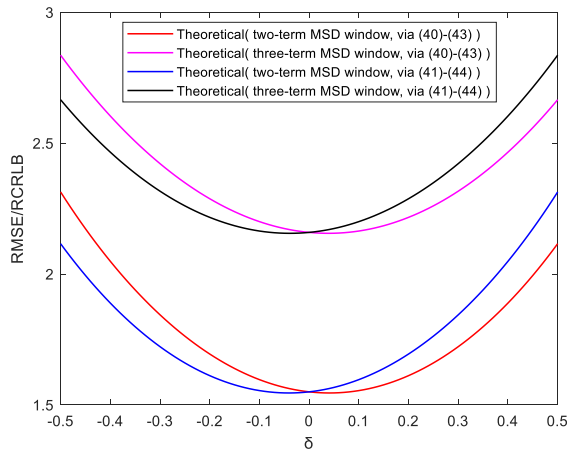


FIGURE 2. Analytical RMSE versus δ ($N = 16$, $SNR=10dB$).

used for comparison include AM estimator [9], HAQSE estimator [12], Candan estimator [19], IpDTFT-NR estimator [20], MV-IPDTFT(2) estimator [21], MV-IPDTFT(3) estimator [21] and PIPDTFT estimator [27]. The AM and HAQSE estimator are based on rectangular window, and the other estimators are based on MSD windows. These experiments are divided into three cases: noisy sinusoid, noisy sinusoid affected by single-tone interfering signal and noisy and harmonically distorted sinusoid. The windows we employ are: the rectangular window ($H = 1$, $a_0 = 1$), the two-term MSD window ($H = 2$, $a_0 = 0.5$ and $a_1 = 0.5$) and three-term MSD window ($H = 3$, $a_0 = 0.375$, $a_1 = 0.5$ and $a_2 = 0.125$). In the simulations, the sinusoid amplitude $A = 1$, the initial phase θ_0 is uniformly distributed on $[0, 2\pi]$.

A. NOISY SINUSOID

When $SNR = 10dB$ and $N = 16$, the theoretical and simulated RMSEs versus the relative frequency deviation δ are shown in Fig. 3. The theoretical RMSEs are calculated

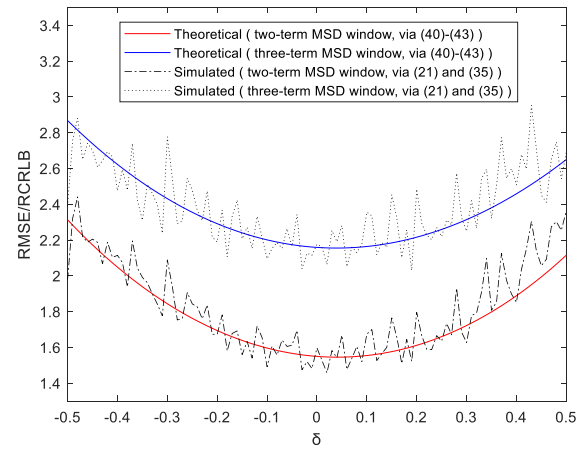


FIGURE 3. Analytical (via (40)-(43)) and simulated (via (21), (35)) RMSEs versus δ ($N = 16$, $SNR=10dB$).

according to (40)-(43). δ varies from -0.5 to 0.5 with a step of 0.01. For each value of δ , 2000 runs are considered. We can see that the theoretical RMSEs are in good agreement with the simulation results.

When all the parameters are the same as Fig. 3, the theoretical and simulated RMSEs versus the relative frequency deviation δ are illustrated in Fig. 4. The theoretical RMSEs are calculated according to (41)-(44). Similar conclusions can be drawn as Fig. 3.

When $SNR = 10dB$ and $N = 16$, Fig. 5 shows the RMSEs of different algorithms with respect to the relative frequency deviation δ . 100,000 runs are considered for each value of δ . It can be observed from Fig. 5 that the RMSE of the presented estimation method by using rectangular window is the lowest and closest to the RCRLB. This is owing to the fact that non-rectangular windowing methods will cause performance degradation when there are no interference signals. The performance of the proposed estimator with

$$\begin{aligned}
 & E \left[(\hat{\delta} - \delta)^2 \right] \\
 & \approx \frac{\left\{ |W_2(0)| \left[\left(\frac{0.2\pi}{N} D - B \right) + \delta \left(\frac{0.2\pi}{N} E - C \right) \right]^2 + 4 |W_2(0)| \cos^2(0.1\pi) \left[\left(\frac{0.1\pi}{N} D - B \right) + \delta \left(\frac{0.1\pi}{N} E - C \right) \right]^2 + |W_2(0)| (B + \delta C)^2 \right\}}{2 \cdot SNR \cdot \left\{ \tilde{W}(0.2 + \delta) \left(\frac{0.2\pi}{N} E - C \right) - 2\tilde{W}(0.1 + \delta) \cos(0.1\pi) \left(\frac{0.1\pi}{N} E - C \right) - \tilde{W}(\delta) C \right\}^2} \\
 & + \frac{\left\{ 4 |W_2(0.1\Delta f)| \cos(0.1\pi) \left[\left(\frac{0.1\pi}{N} D - B \right) + \delta \left(\frac{0.1\pi}{N} E - C \right) \right] (B + \delta C) - 2 |W_2(0.2\Delta f)| \left[\left(\frac{0.2\pi}{N} D - B \right) + \delta \left(\frac{0.2\pi}{N} E - C \right) \right] (B + \delta C) \right\}}{2 \cdot SNR \cdot \left\{ \tilde{W}(0.2 + \delta) \left(\frac{0.2\pi}{N} E - C \right) - 2\tilde{W}(0.1 + \delta) \cos(0.1\pi) \left(\frac{0.1\pi}{N} E - C \right) - \tilde{W}(\delta) C \right\}^2} \\
 & - \frac{\left\{ 4 |W_2(0.1\Delta f)| \cos(0.1\pi) \left[\left(\frac{0.2\pi}{N} D - B \right) + \delta \left(\frac{0.2\pi}{N} E - C \right) \right] \left[\left(\frac{0.1\pi}{N} D - B \right) + \delta \left(\frac{0.1\pi}{N} E - C \right) \right] \right\}}{2 \cdot SNR \cdot \left\{ \tilde{W}(0.2 + \delta) \left(\frac{0.2\pi}{N} E - C \right) - 2\tilde{W}(0.1 + \delta) \cos(0.1\pi) \left(\frac{0.1\pi}{N} E - C \right) - \tilde{W}(\delta) C \right\}^2} \tag{44}
 \end{aligned}$$

$$E \left[\left(\hat{\delta}_{w1} - \delta \right)^2 \right] = \frac{|W_2(0)| \left[\frac{\pi^2 \rho^2}{N^2} + \delta^2 + 2\delta^2 \right] - |W_2(2\Delta f)| \left(\frac{\pi^2 \rho^2}{N^2} - \delta^2 \right) + 4 |W_2(\Delta f)| \delta^2}{SNR \cdot \left[\tilde{W}(1 - \delta) + \tilde{W}(1 + \delta) + 2\tilde{W}(\delta) \right]^2} \tag{45}$$

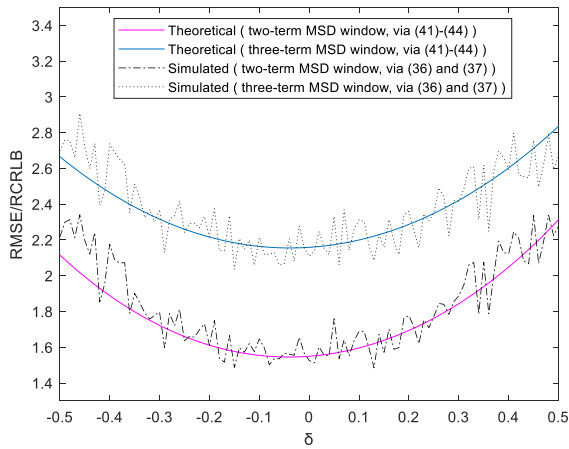


FIGURE 4. Analytical (via (41)-(44)) and simulated (via (36), (37)) RMSEs versus δ ($N = 16, SNR=10dB$).

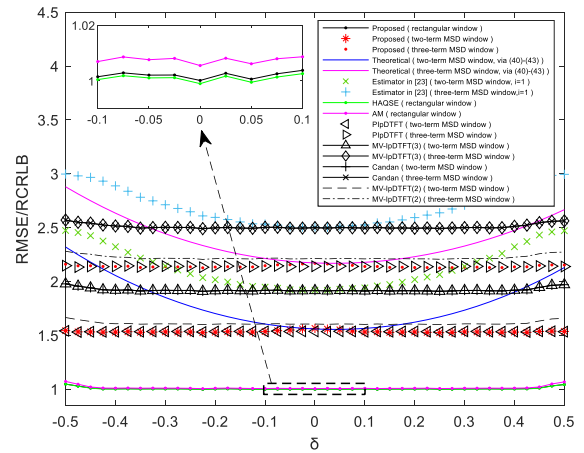


FIGURE 6. RMSEs of different algorithms versus δ ($N = 128, SNR=3dB$).

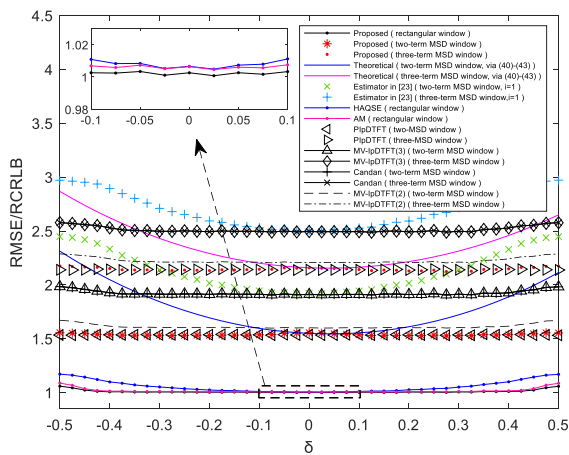


FIGURE 5. RMSEs of different algorithms versus δ ($N = 16, SNR=10dB$).

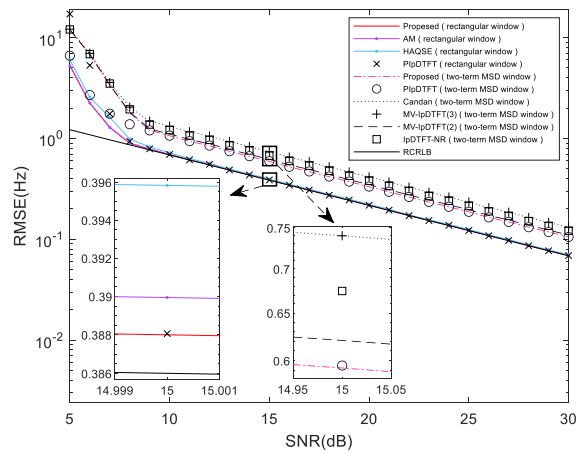


FIGURE 7. RMSEs of different algorithms with two-term MSD window versus SNR ($N = 16, \delta=0.2$).

two-term MSD window and the PIPDFT estimator with two-term MSD window are very close to each other. These two estimators achieve better results than the other windowing methods. It can also be seen that the RMSEs of the estimator in [23] (used in the preliminary estimation) increase with the increase of $|\delta|$ and are relatively bigger than the other methods with the same window. The RMSEs of the proposed estimator based on MSD windows are almost independent of δ and are very close to the theoretical minimum values returned by (40).

When $SNR = 3dB$ and $N = 128$, the RMSEs of different algorithms versus δ are shown in Fig. 6. 100,000 runs are considered for each value of δ . We can see from Fig. 6 that the RMSE of the proposed method with rectangular window is lower than that of AM method, and higher than that of HAQSE method. The performance of the presented method with two-term MSD window and the PIPDFT estimator with two-term MSD window are very close to each other. The RMSEs of these two estimators are lower than those of the other windowing methods. The RMSEs of the presented method based on MSD windows are almost independent of δ

and are very close to the theoretical minimum values returned by (40).

Fig. 7 compares the RMSEs of different estimators with two-term MSD window versus SNR when $N = 16$ and $\delta = 0.2$. 20,000 runs are considered for each value of SNR. We can see that the presented algorithm with rectangular window is the closest to the RCRLB. Among all the algorithms with two-term MSD window, the presented algorithm can achieve the best results.

When all the parameters are the same as Fig. 7, the RMSEs versus SNR of various algorithms with three-term MSD window are shown in Fig. 8. Similar conclusions can be drawn as Fig. 7.

B. NOISY SINUSOID AFFECTED BY SINGLE-TONE INTERFERING SIGNAL

Next, the case of noisy sinusoid affected by single-tone interfering signal is considered. It is assumed the frequency of the single-tone interference sinusoid is $6\Delta f$ higher than that of the sinusoid to be estimated, and the SIR (signal-to-interference ratio) is 3dB. The initial phase of the interfering

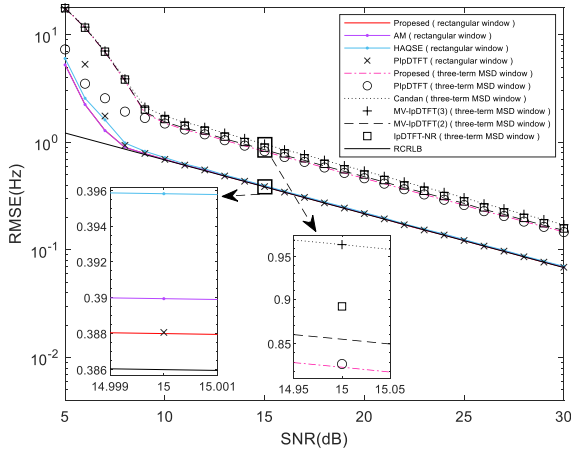


FIGURE 8. RMSEs of different algorithms with three-term MSD window versus SNR ($N = 16, \delta = 0.2$).

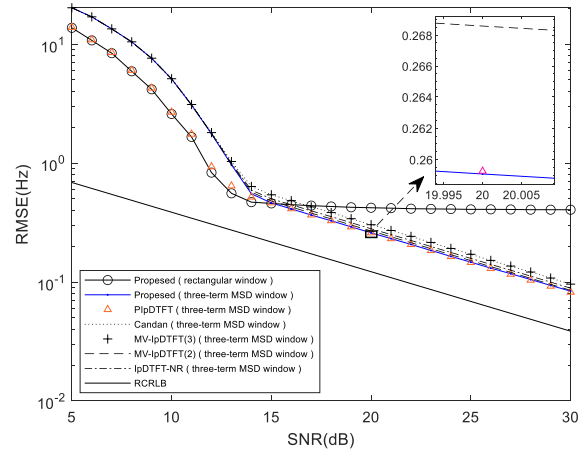


FIGURE 10. RMSEs of different algorithms with three-term MSD window versus SNR ($N = 16, \delta = 0.2, SIR = 3dB$).

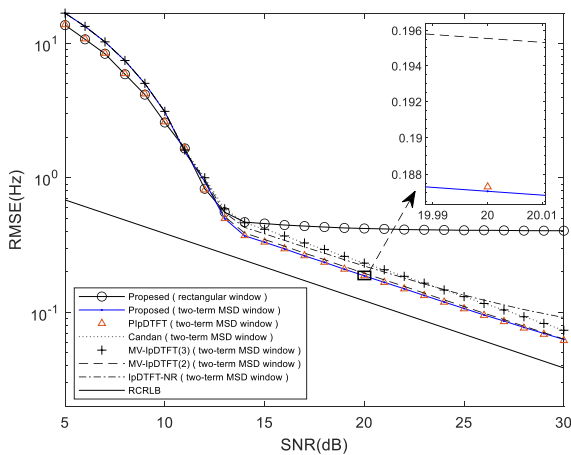


FIGURE 9. RMSEs of different algorithms with two-term MSD window versus SNR ($N = 16, \delta = 0.2, SIR = 3dB$).

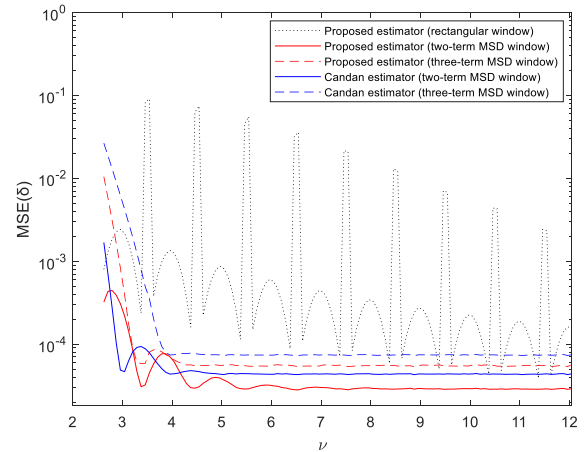


FIGURE 11. MSEs of the presented and Candan estimator versus the number of observed cycles ν ($N = 128, SNR = 20dB, THD = 60%$).

signal is uniformly distributed on $[0, 2\pi]$. 20,000 runs are considered for each value of SNR .

When $N = 16$ and $\delta = 0.2$, the RMSEs versus SNR of various algorithms are shown in Fig. 9. It can be noted that the RMSE of the presented estimation method by using two-term MSD window is closer to the RCRLB than the other algorithms. When the SNR is higher than 15dB, the presented algorithm based on rectangular window gradually moves away from the RCRLB. Therefore, when single-tone interfering signal exists besides white noise, windowing methods can reduce the impact of the interference sinusoid on the desired sinusoid.

The RMSEs versus SNR of various methods by using three-term MSD window are illustrated in Fig. 10. When all the parameters are the same as Fig. 9, Fig. 10 illustrates that the performance of the presented algorithm based on three-term MSD window is better than that of the other methods based on three-term MSD window and the presented method with rectangular window. Therefore, when

single-tone interfering sinusoid exists besides white noise, windowing methods have to be preferred.

C. NOISY AND HARMONICALLY DISTORTED SINUSOID

In the simulations of this part, it is assumed that there are the 2nd, 3rd and 4th harmonics. And the amplitude ratios of the harmonics are 4:2:1. We assume that the Total harmonic Distortion (THD) is equal to 60%. The initial phases of the harmonics are uniformly distributed on $[0, 2\pi]$. The value of the number of observed cycles ν varies in $[2.54, 12.04]$ and the step is $1/12$. For each value of ν , 20,000 runs are considered.

Fig. 11 illustrates the MSEs of the presented and Candan estimator versus ν when $N = 128, SNR = 20dB$. When ν is in range of $[2.75, 3.21]$ or $[3.65, 4.15]$, it is noticed that the MSE of Candan estimator based on two-term MSD window is lower than that of the other methods. And we also observe that the MSE of the presented algorithm is lower than that of the other windowing methods when ν is in range of $[3.21, 3.65]$ or $[4.15, 12.04]$. We can see evidently from

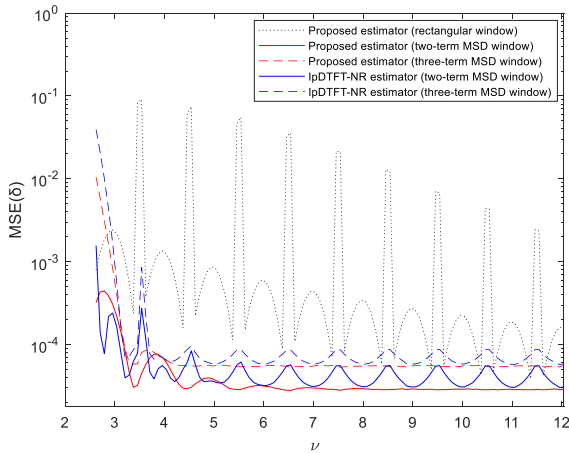


FIGURE 12. MSEs of presented and IpDTFT-NR estimator versus ν ($N = 128, SNR = 20dB, THD = 60\%$).

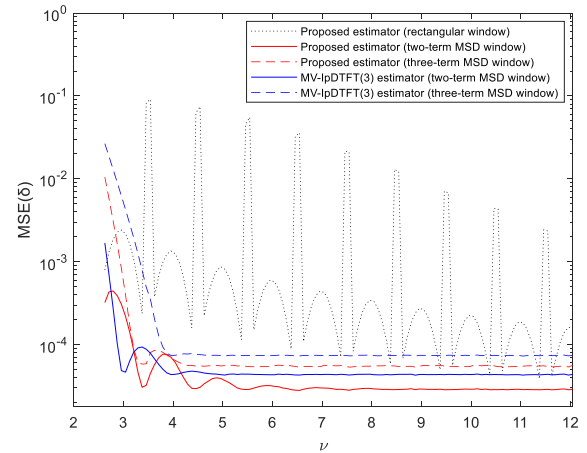


FIGURE 14. MSEs of the presented and MV-IPDTFT(3) estimator versus ν ($N = 128, SNR = 20dB, THD = 60\%$).

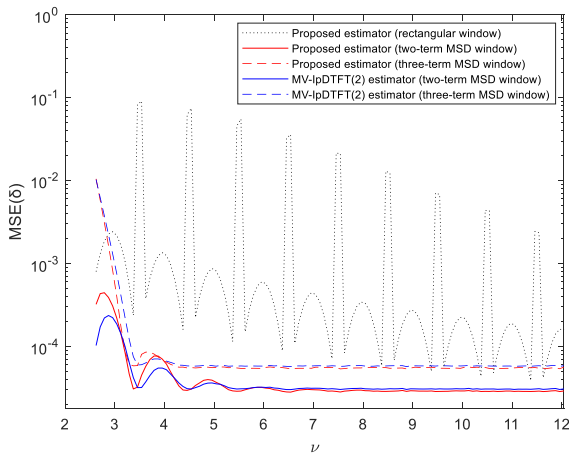


FIGURE 13. MSEs of the presented and MV-IPDTFT(2) estimator versus ν ($N = 128, SNR = 20dB, THD = 60\%$).

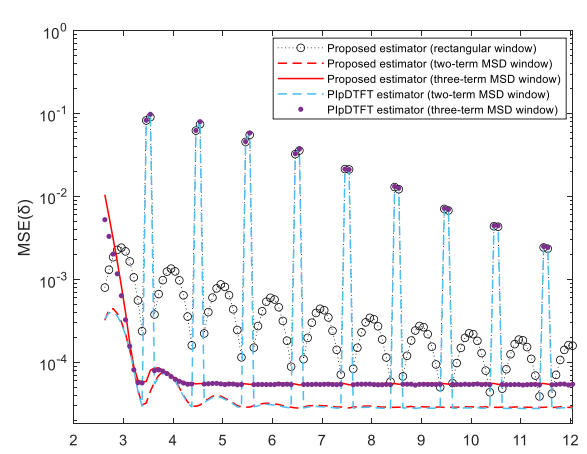


FIGURE 15. MSEs of the presented and PIPDTFT estimator versus ν ($N = 128, SNR = 20dB, THD = 60\%$).

Fig. 11 that the presented algorithm with rectangular window fluctuates greatly. For the same algorithm, the estimation performance with two-term MSD is better than that based on three-term MSD window. As ν increases, the performance of the estimation methods by using MSD windows gradually tend to be stable.

The performance of estimator in this paper and IpDTFT-NR estimator are illustrated in Fig. 12 for $N = 128$, $SNR = 20dB$. As can be noted from Fig. 12, the performance of the presented estimator by using two-term MSD window outperforms the other windowing estimators when $\nu \geq 5.14$. When $\nu < 5.14$, the presented estimator with two-term MSD window and IpDTFT-NR estimator with two-term MSD window can alternately achieve better results than the other algorithms.

Fig. 13 shows the MSEs of the presented and MV-IPDTFT(2) estimator versus ν when $N = 128$ and $SNR = 20dB$. We can obtain that the presented method with two-term MSD window and MV-IPDTFT(2) method with two-term MSD window can alternately achieve better

results than the other algorithms when $\nu < 5.12$. When $\nu \geq 5.12$, the MSE of the algorithm we present by using two-term MSD window is lower than the other windowing methods and should be preferred. The MSE of the presented rectangular windowing method fluctuates greatly. And it is worth noting that the estimation method with two-term MSD window achieves better results than the same method with three-term MSD window.

Fig. 14 shows the MSEs of the presented and MV-IPDTFT(3) estimator versus ν for $N = 128$, $SNR = 20dB$. When all the simulation parameters are the same as Fig. 11, it can be seen that the performance of MV-IPDTFT(3) method is very close to that of Candan method. Therefore, we can obtain similar conclusions as Fig. 11.

When $N = 128$ and $SNR = 20dB$, the MSEs of the presented and PIPDTFT estimator versus ν are shown in Fig. 15. We can see that the performance of the PIPDTFT method is poor when $|\delta|$ is close to 0.5. The MSE of the presented rectangular windowing method fluctuates greatly.

TABLE 2. Computational requirements of different estimators.

Estimators	Complex multiplications	Complex additions
Proposed	$(N/2)\log_2 N + 3N$	$N \log_2 N + 3N - 3$
AM [9]	$(N/2)\log_2 N + 4N + 2$	$N \log_2 N + 4N$
HAQSE [12]	$(N/2)\log_2 N + 4N + 2$	$N \log_2 N + 4N$
Candan [19]	$(N/2)\log_2 N + 3N + 2$	$N \log_2 N + 3N + 3$
MV-IPDTFT(3) [21]	$(N/2)\log_2 N + 3N + 2$	$N \log_2 N + 3N + 3$
IPDTFT-NR [20]	$(N/2)\log_2 N + 8N + 1$	$N \log_2 N + 8N - 6$
MV-IPDTFT(2) [21]	$(N/2)\log_2 N + 4N$	$N \log_2 N + 4N - 4$
PIpDTFT [27]	$(N/2)\log_2 N + 3N$	$N \log_2 N + 3N$

The proposed method with two-term MSD window achieves better results than the other algorithms.

The computational requirements of different estimators are given in Table. 2. The AM estimator [9], HAQSE estimator [12], Candan estimator [19], MV-IPDTFT(3) estimator [21], IPDTFT-NR [20] and MV-IPDTFT(2) estimator [21] are used in the second iteration. The computational requirements of the proposed method are almost the same with those of Candan, MV-IPDTFT(3) and PIpDTFT estimator [27], and are lower than those of the other estimators.

IV. CONCLUSION

A sinusoidal signal frequency estimator based on interpolated DFT by using MSD window is proposed in this paper. The received sinusoid is multiplied with MSD windows to reduce the impact of the interference signals on the frequency estimation. The maximum DFT sample and two DTFT spectrum lines which are on the same side of the maximum DFT sample are utilized in the fine estimation step. MSE formulas of the presented estimator in additive white noise are derived. The simulation results show that under the circumstances of noisy sinusoid affected by single-tone interfering signal, and noisy and harmonically distorted sinusoid, the estimation method presented in this paper achieves better results than Candan method, IPDTFT-NR method, MV-IPDTFT(2) method, MV-IPDTFT(3) method and PIpDTFT estimator. The impact of the interference signals on the frequency estimation of the received sinusoid can be reduced by using the presented method. The computational complexity of the proposed method is almost the same with that of Candan, MV-IPDTFT (3) and PIpDTFT estimator, and is lower than that of the other competing estimators.

APPENDIX

The MSE formula of $\hat{\delta}$ via (35) and (21) in the background of additive white noise is deduced firstly.

The amplitude of the DTFT of $x_w[n]$ is expressed as [23]

$$|X_f| \approx A_f + \text{Re} \left(Z_f e^{-j\phi_f} \right) = A_f + U_f \quad (46)$$

where A_f , ϕ_f are the amplitude and phase of the DTFT of $s_w[n]$. Z_f is the DTFT of $z_w[n]$ and U_f is the real part of $Z_f e^{-j\phi_f}$.

For the convenience of expression, when $f = m\Delta f$, $(m + 0.1)\Delta f$ and $(m + 0.2)\Delta f$, the amplitudes of the three spectral lines $|X_{m\Delta f}|$, $|X_{(m+0.1)\Delta f}|$ and $|X_{(m+0.2)\Delta f}|$ are denoted as $|X_0|$, $|X_{0.1}|$ and $|X_{0.2}|$. Then we can get

$$|X_0| \approx A_{m\Delta f} + U_{m\Delta f} = A_0 + U_0 \quad (47)$$

$$|X_{0.1}| \approx A_{(m+0.1)\Delta f} + U_{(m+0.1)\Delta f} = A_{0.1} + U_{0.1} \quad (48)$$

$$|X_{0.2}| \approx A_{(m+0.2)\Delta f} + U_{(m+0.2)\Delta f} = A_{0.2} + U_{0.2} \quad (49)$$

where $A_{m\Delta f}$, $A_{(m+0.1)\Delta f}$ and $A_{(m+0.2)\Delta f}$ are denoted as A_0 , $A_{0.1}$ and $A_{0.2}$ respectively. $U_{m\Delta f}$, $U_{(m+0.1)\Delta f}$ and $U_{(m+0.2)\Delta f}$ are denoted as U_0 , $U_{0.1}$ and $U_{0.2}$ respectively.

In additive noise background, we replace $|S_w(m)|$, $|S_w(m + 0.1)|$ and $|S_w(m + 0.2)|$ in (21) with $|X_0|$, $|X_{0.1}|$ and $|X_{0.2}|$. Then we have

$$Y = \frac{|X_{0.2}| \sin \left(\frac{0.2\pi}{N} \right) - 2 |X_{0.1}| \sin \left(\frac{0.1\pi}{N} \right) \cos (0.1\pi)}{|X_0| + |X_{0.2}| \cos \left(\frac{0.2\pi}{N} \right) - 2 |X_{0.1}| \cos \left(\frac{0.1\pi}{N} \right) \cos (0.1\pi)} \quad (50)$$

Then (35) can be written as

$$\hat{\delta} = \frac{YD - B}{YE - C} = \frac{L_1 D - L_2 B}{L_1 E - L_2 C} \quad (51)$$

where L_1 and L_2 are the numerator and denominator of Y respectively. Then the numerator of $\hat{\delta}$ can be written as

$$\begin{aligned} & L_1 D - L_2 B \\ &= \left[|X_{0.2}| \sin \left(\frac{0.2\pi}{N} \right) - 2 |X_{0.1}| \sin \left(\frac{0.1\pi}{N} \right) \cos (0.1\pi) \right] D \\ &\quad - \left[|X_0| + |X_{0.2}| \cos \left(\frac{0.2\pi}{N} \right) \right. \\ &\quad \left. - 2 |X_{0.1}| \cos \left(\frac{0.1\pi}{N} \right) \cos (0.1\pi) \right] B \end{aligned} \quad (52)$$

By substituting (47)-(49) into (52) and we have

$$\begin{aligned} & L_1 D - L_2 B \\ &= \left[A_{0.2} \left(\sin \left(\frac{0.2\pi}{N} \right) D - \cos \left(\frac{0.2\pi}{N} \right) B \right) \right. \\ &\quad \left. - 2A_{0.1} \cos (0.1\pi) \left(\sin \left(\frac{0.1\pi}{N} \right) D - \cos \left(\frac{0.1\pi}{N} \right) C \right) \right. \\ &\quad \left. - A_0 B \right] \\ &\quad + \left[U_{0.2} \left(\sin \left(\frac{0.2\pi}{N} \right) D - \cos \left(\frac{0.2\pi}{N} \right) B \right) \right. \\ &\quad \left. - 2U_{0.1} \cos (0.1\pi) \left(\sin \left(\frac{0.1\pi}{N} \right) D - \cos \left(\frac{0.1\pi}{N} \right) C \right) \right. \\ &\quad \left. - U_0 B \right] \end{aligned} \quad (53)$$

Similarly, the denominator of (51) can be expressed as

$$\begin{aligned}
 &L_1E - L_2C \\
 &= \left[A_{0.2} \left(\sin \left(\frac{0.2\pi}{N} \right) E - \cos \left(\frac{0.2\pi}{N} \right) C \right) \right. \\
 &\quad - 2A_{0.1} \cos(0.1\pi) \left(\sin \left(\frac{0.1\pi}{N} \right) E \right. \\
 &\quad \left. \left. - \cos \left(\frac{0.1\pi}{N} \right) C \right) - A_0C \right] \\
 &+ \left[U_{0.2} \left(\sin \left(\frac{0.2\pi}{N} \right) E - \cos \left(\frac{0.2\pi}{N} \right) C \right) \right. \\
 &\quad - 2U_{0.1} \cos(0.1\pi) \left(\sin \left(\frac{0.1\pi}{N} \right) E \right. \\
 &\quad \left. \left. - \cos \left(\frac{0.1\pi}{N} \right) C \right) - U_0C \right] \tag{54}
 \end{aligned}$$

Substituting (53) and (54) into (51), after some derivation in (55), as shown at the top of the previous page.

Under high SNR, we derived in (56), as shown at the top of the previous page.

The equation (55) is expanded by the first order Taylor series and the higher-order terms are ignored. Then we derived in (57), as shown at the top of the previous page.

Under high SNR, the third term is much larger than the fourth term in (57). Therefore, we ignore the fourth term in the above equation and can obtain in (58), as shown at the top of the previous page.

Using $A_0 = S_w(m)$, $A_{0.1} = S_w(m+0.1)$ and $A_{0.2} = S_w(m+0.2)$ in (35), we get in (59), as shown at the bottom of the page.

Substituting (59) in (58), we derived in (60), as shown at the bottom of the page.

Formula (60) can be written in (61), as shown at the bottom of the page.

When N is much larger than 1, we have $\cos(0.2\pi/N) \approx 1$, $\cos(0.1\pi/N) \approx 1$, $\sin(0.2\pi/N) \approx 0.2\pi/N$ and $\sin(0.1\pi/N) \approx 0.1\pi/N$. Then we can obtain in (62), as shown at the bottom of the page.

We consider the denominator of (62) first. As A_i can be expressed as $A_i = A\tilde{W}(i - \delta)$ and $\tilde{W}(\cdot)$ is an even function, we can obtain

$$\begin{aligned}
 &\left[A_{0.2} \left(\frac{0.2\pi}{N} E - C \right) \right. \\
 &\quad \left. - 2A_{0.1} \cos(0.1\pi) \left(\frac{0.1\pi}{N} E - C \right) - A_0C \right]^2 \\
 &= A^2 \left[\tilde{W}(0.2 - \delta) \left(\frac{0.2\pi}{N} E - C \right) \right. \\
 &\quad \left. - 2\tilde{W}(0.1 - \delta) \cos(0.1\pi) \left(\frac{0.1\pi}{N} E - C \right) - \tilde{W}(\delta) C \right]^2 \tag{63}
 \end{aligned}$$

Then we consider the numerator of (62) as follows

$$\begin{aligned}
 &E \left\{ \left[U_{0.2} \left(\left(\frac{0.2\pi}{N} D - B \right) - \delta \left(\frac{0.2\pi}{N} E - C \right) \right) \right. \right. \\
 &\quad \left. \left. - 2U_{0.1} \cos(0.1\pi) \left(\left(\frac{0.1\pi}{N} D - B \right) \right) \right] \right\}
 \end{aligned}$$

$$\delta = \frac{A_{0.2} \left(\sin \left(\frac{0.2\pi}{N} \right) D - \cos \left(\frac{0.2\pi}{N} \right) B \right) - 2A_{0.1} \cos(0.1\pi) \left(\sin \left(\frac{0.1\pi}{N} \right) D - \cos \left(\frac{0.1\pi}{N} \right) B \right) - A_0B}{A_{0.2} \left(\sin \left(\frac{0.2\pi}{N} \right) E - \cos \left(\frac{0.2\pi}{N} \right) C \right) - 2A_{0.1} \cos(0.1\pi) \left(\sin \left(\frac{0.1\pi}{N} \right) E - \cos \left(\frac{0.1\pi}{N} \right) C \right) - A_0C} \tag{59}$$

$$\begin{aligned}
 \hat{\delta} &= \delta + \frac{U_{0.2} \left(\sin \left(\frac{0.2\pi}{N} \right) D - \cos \left(\frac{0.2\pi}{N} \right) B \right) - 2U_{0.1} \cos(0.1\pi) \left(\sin \left(\frac{0.1\pi}{N} \right) D - \cos \left(\frac{0.1\pi}{N} \right) B \right) - U_0B}{A_{0.2} \left(\sin \left(\frac{0.2\pi}{N} \right) E - \cos \left(\frac{0.2\pi}{N} \right) C \right) - 2A_{0.1} \cos(0.1\pi) \left(\sin \left(\frac{0.1\pi}{N} \right) E - \cos \left(\frac{0.1\pi}{N} \right) C \right) - A_0C} \\
 &\quad - \delta \frac{U_{0.2} \left(\sin \left(\frac{0.2\pi}{N} \right) E - \cos \left(\frac{0.2\pi}{N} \right) C \right) - 2U_{0.1} \cos(0.1\pi) \left(\sin \left(\frac{0.1\pi}{N} \right) E - \cos \left(\frac{0.1\pi}{N} \right) C \right) - U_0C}{A_{0.2} \left(\sin \left(\frac{0.2\pi}{N} \right) E - \cos \left(\frac{0.2\pi}{N} \right) C \right) - 2A_{0.1} \cos(0.1\pi) \left(\sin \left(\frac{0.1\pi}{N} \right) E - \cos \left(\frac{0.1\pi}{N} \right) C \right) - A_0C} \tag{60}
 \end{aligned}$$

$$\begin{aligned}
 \hat{\delta} - \delta &= \frac{U_{0.2} \left[\left(\sin \left(\frac{0.2\pi}{N} \right) D - \cos \left(\frac{0.2\pi}{N} \right) B \right) - \delta \left(\sin \left(\frac{0.2\pi}{N} \right) E - \cos \left(\frac{0.2\pi}{N} \right) C \right) \right] - U_0(B - \delta C)}{A_{0.2} \left(\sin \left(\frac{0.2\pi}{N} \right) E - \cos \left(\frac{0.2\pi}{N} \right) C \right) - 2A_{0.1} \cos(0.1\pi) \left(\sin \left(\frac{0.1\pi}{N} \right) E - \cos \left(\frac{0.1\pi}{N} \right) C \right) - A_0C} \\
 &\quad - \frac{2U_{0.1} \cos(0.1\pi) \left[\left(\sin \left(\frac{0.1\pi}{N} \right) D - \cos \left(\frac{0.1\pi}{N} \right) B \right) - \delta \left(\sin \left(\frac{0.1\pi}{N} \right) E - \cos \left(\frac{0.1\pi}{N} \right) C \right) \right]}{A_{0.2} \left(\sin \left(\frac{0.2\pi}{N} \right) E - \cos \left(\frac{0.2\pi}{N} \right) C \right) - 2A_{0.1} \cos(0.1\pi) \left(\sin \left(\frac{0.1\pi}{N} \right) E - \cos \left(\frac{0.1\pi}{N} \right) C \right) - A_0C} \tag{61}
 \end{aligned}$$

$$E \left[\left(\hat{\delta} - \delta \right)^2 \right] = \frac{E \left\{ \left[U_{0.2} \left(\left(\frac{0.2\pi}{N} D - B \right) - \delta \left(\frac{0.2\pi}{N} E - C \right) \right) - 2U_{0.1} \cos(0.1\pi) \left(\left(\frac{0.1\pi}{N} D - B \right) - \delta \left(\frac{0.1\pi}{N} E - C \right) \right) - U_0(B - \delta C) \right]^2 \right\}}{\left[A_{0.2} \left(\frac{0.2\pi}{N} E - C \right) - 2A_{0.1} \cos(0.1\pi) \left(\frac{0.1\pi}{N} E - C \right) - A_0C \right]^2} \tag{62}$$

$$\begin{aligned}
& -\delta \left(\frac{0.1\pi}{N} E - C \right) - U_0 (B - \delta C) \Big]^2 \Big\} \\
= & E \left\{ U_{0.2}^2 \left[\left(\frac{0.2\pi}{N} D - B \right) - \delta \left(\frac{0.2\pi}{N} E - C \right) \right]^2 \right. \\
& + 4U_{0.1}^2 \cos^2(0.1\pi) \left[\left(\frac{0.1\pi}{N} D - B \right) - \delta \left(\frac{0.1\pi}{N} E - C \right) \right]^2 \\
& + U_0^2 (B - \delta C)^2 \\
& - 2U_{0.2}U_0 \left[\left(\frac{0.2\pi}{N} D - B \right) - \delta \left(\frac{0.2\pi}{N} E - C \right) \right] (B - \delta C) \\
& + 4U_0U_{0.1} \cos(0.1\pi) \left[\left(\frac{0.1\pi}{N} D - B \right) - \delta \left(\frac{0.1\pi}{N} E - C \right) \right] \\
& (B - \delta C) \\
& - 4U_{0.2}U_{0.1} \cos(0.1\pi) \left[\left(\frac{0.1\pi}{N} D - B \right) \right. \\
& \left. - \delta \left(\frac{0.1\pi}{N} E - C \right) \right] \left[\left(\frac{0.2\pi}{N} D - B \right) \right. \\
& \left. - \delta \left(\frac{0.2\pi}{N} E - C \right) \right] \Big\} \quad (64)
\end{aligned}$$

The autocorrelation function of U_f is [23]

$$\begin{aligned}
E(U_{f_1}, U_{f_2}) &= \frac{\sigma^2}{2} |W_2(f_1 - f_2)| \\
&= \frac{\sigma^2}{2} \sum_{n=0}^{N-1} w^2(n) e^{-j2\pi(f_1 - f_2)Tn/N} \quad (65)
\end{aligned}$$

Then we have

$$E(U_{0.2}U_0) = \frac{\sigma^2}{2} |W_2(0.2\Delta f)| \quad (66)$$

$$E(U_{0.2}U_{0.1}) = E(U_{0.1}U_0) = \frac{\sigma^2}{2} |W_2(0.1\Delta f)| \quad (67)$$

$$E(U_0^2) = E(U_{0.1}^2) = E(U_{0.2}^2) = \frac{\sigma^2}{2} |W_2(0)| \quad (68)$$

By substituting (63)-(68) into (62), we obtain the MSE formula (40).

After similar derivation, the MSE formula of $\hat{\delta}$ via (36) and (37) can be obtained as (44).

REFERENCES

- [1] D. C. Rife and R. R. Boorstyn, "Single tone parameter estimation from discrete-time observations," *IEEE Trans. Inf. Theory*, vol. IT-20, no. 5, pp. 591-598, Sep. 1974.
- [2] A. J. S. Dutra, J. F. L. de Oliveira, T. M. Prego, S. L. Netto, and E. A. B. da Silva, "High-precision frequency estimation of real sinusoids with reduced computational complexity using a model-based matched-spectrum approach," *Digit. Signal Process.*, vol. 34, pp. 67-73, Nov. 2014.
- [3] C. Candan and U. Çelebi, "Frequency estimation of a single real-valued sinusoid: An invariant function approach," *Signal Process.*, vol. 185, Aug. 2021, Art. no. 108098.
- [4] R. Elasmî-Ksibi, H. Besbes, R. López-Valcarce, and S. Cherif, "Frequency estimation of real-valued single-tone in colored noise using multiple autocorrelation lags," *Signal Process.*, vol. 90, no. 7, pp. 2303-2307, Jul. 2010.
- [5] C. Yang and W. Wei, "A noniterative frequency estimator with rational combination of three spectrum lines," *IEEE Trans. Signal Process.*, vol. 59, no. 10, pp. 5065-5070, Oct. 2011.
- [6] Y. Cao, G. Wei, and F.-J. Chen, "A closed-form expanded autocorrelation method for frequency estimation of a sinusoid," *Signal Process.*, vol. 92, no. 4, pp. 885-892, Apr. 2012.
- [7] Y. Q. Tu and Y. L. Shen, "Phase correction autocorrelation-based frequency estimation method for sinusoidal signal," *Signal Process.*, vol. 130, no. 1, pp. 183-189, Jan. 2017.
- [8] D. W. Tufts and R. Kumaresan, "Estimation of frequencies of multiple sinusoids: Making linear prediction perform like maximum likelihood," *Proc. IEEE*, vol. 70, no. 9, pp. 975-989, Sep. 1982.
- [9] E. Aboutanios and B. Mulgrew, "Iterative frequency estimation by interpolation on Fourier coefficients," *IEEE Trans. Signal Process.*, vol. 53, no. 4, pp. 1237-1242, Apr. 2005.
- [10] C. Candan, "A method for fine resolution frequency estimation from three DFT samples," *IEEE Signal Process. Lett.*, vol. 18, no. 6, pp. 351-354, Jun. 2011.
- [11] J.-R. Liao and C.-M. Chen, "Phase correction of discrete Fourier transform coefficients to reduce frequency estimation bias of single tone complex sinusoid," *Signal Process.*, vol. 94, pp. 108-117, Jan. 2014.
- [12] A. Serbes, "Fast and efficient sinusoidal frequency estimation by using the DFT coefficients," *IEEE Trans. Commun.*, vol. 67, no. 3, pp. 2333-2342, Mar. 2019.
- [13] L. Fan and G. Qi, "Frequency estimator of sinusoid based on interpolation of three DFT spectral lines," *Signal Process.*, vol. 144, pp. 52-60, Mar. 2018.
- [14] U. Orguner and C. Candan, "A fine-resolution frequency estimator using an arbitrary number of DFT coefficients," *Signal Process.*, vol. 105, no. 10, pp. 17-21, Dec. 2014.
- [15] X. H. Liang, A. J. Liu, X. F. Pan, Q. S. Zhang, and F. Chen, "A new and accurate estimator with analytical expression for frequency estimation," *IEEE Commun. Lett.*, vol. 20, no. 1, pp. 105-108, Jan. 2016.
- [16] A. Serbes and K. Qaraqe, "A fast method for estimating frequencies of multiple sinusoids," *IEEE Signal Process. Lett.*, vol. 27, pp. 386-390, 2020.
- [17] K. Wang, L. Zhang, H. Wen, and L. Xu, "A sliding-window DFT based algorithm for parameter estimation of multi-frequency signal," *Digit. Signal Process.*, vol. 97, Feb. 2020, Art. no. 102617.
- [18] L. Fan, G. Qi, J. Xing, J. Jin, J. Liu, and Z. Wang, "Accurate frequency estimator of sinusoid based on interpolation of FFT and DTFT," *IEEE Access*, vol. 8, pp. 44373-44380, 2020.
- [19] Ç. Candan, "Fine resolution frequency estimation from three DFT samples: Case of windowed data," *Signal Process.*, vol. 114, pp. 245-250, Sep. 2015.
- [20] D. Belega, D. Petri, and D. Dallet, "Accurate frequency estimation of a noisy sine-wave by means of an interpolated discrete-time Fourier transform algorithm," *Measurement*, vol. 116, pp. 685-691, Feb. 2018.
- [21] D. Belega and D. Petri, "Frequency estimation by two-or three-point interpolated Fourier algorithms based on cosine windows," *Signal Process.*, vol. 117, pp. 115-125, Dec. 2015.
- [22] D. Belega and D. Petri, "Fast procedures for accurate parameter estimation of sine-waves affected by noise and harmonic distortion," *Digit. Signal Process.*, vol. 114, Jul. 2021, Art. no. 103035.
- [23] L. Fan, G. Q. Qi, J. Y. Liu, J. Y. Jin, L. Liu, and J. Xing, "Frequency estimator of sinusoid by interpolated DFT method based on maximum sidelobe decay windows," *Signal Process.*, vol. 186, Sep. 2021, Art. no. 108125.
- [24] D. Shin, C. Kwak, and G. Kim, "An efficient algorithm for frequency estimation from cosine-sum windowed DFT coefficients," *Signal Process.*, vol. 166, Jul. 2020, Art. no. 107245.
- [25] D. Belega and D. Petri, "Effect of noise and harmonics on sine-wave frequency estimation by interpolated DFT algorithms based on few observed cycles," *Signal Process.*, vol. 140, pp. 207-218, Nov. 2017.
- [26] K. Duda and S. Barczentewicz, "Interpolated DFT for $\sin^a(x)$ windows," *IEEE Trans. Instrum. Meas.*, vol. 63, no. 4, pp. 754-760, Apr. 2014.
- [27] D. Belega and D. Petri, "Unbiased sine-wave frequency estimation by parabolic interpolation of DTFT samples," Presented at the IEEE Int. Instrum. Meas. Technol. Conf., Glasgow, U.K., Jun. 2021.

- [28] J. Borkowski, J. Mroczka, A. Matusiak, and K. Dairus, "Frequency estimation in interpolated discrete Fourier transform with generalized maximum sidelobe decay windows for the control of power," *IEEE Trans. Ind. Informat.*, vol. 17, no. 3, pp. 1614–1624, Mar. 2021.



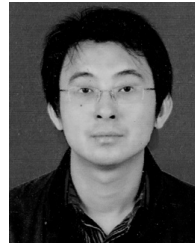
HUIHAO WU was born in 1998. He received the bachelor's degree in communication engineering from Qingdao Agricultural University (QAU), in 2021. He is currently pursuing the master's degree with Dalian Polytechnic University (DLPU), China. His research interests include parameter estimation and signal detection.



HUANHUAN SONG was born in 1998. She received the bachelor's degree in communication engineering from Dalian Polytechnic University (DLPU), China, in 2021, where she is currently pursuing the master's degree. Her research interests include parameter estimation and signal detection.



YUCHAN BAI was born in Siping, China. She received the bachelor's degree in communication engineering from the School of Information Science and Engineering, Dalian Polytechnic University (DLPU). Her research interests include signal detection and parameter estimation.



LEI FAN was born in 1980. He received the B.Sc., M.Sc., and Ph.D. degrees in information and communication engineering from Dalian Maritime University, in 2003, 2006, and 2018, respectively. He is currently a Lecturer with the School of Information Science and Engineering, Dalian Polytechnic University, China. His research interests include parameter estimation, signal detection, and signal processing.



JIYOU JIN received the Ph.D. degree in information and communication engineering from Yeungnam University, Gyeongsan, Republic of Korea, in 2007. From 2007 to 2008, he was a Postdoctoral Researcher with the School of Electrical Engineering and Computer Science, Seoul National University, Republic of Korea. From 2008 to 2009, he was an Assistant Professor of information and communication engineering with Yeungnam University. He joined as a Technical Director with Hilandwe Communication Technology Company Ltd., in 2010. He is currently an Associate Professor with the School of Information Science and Engineering, Dalian Polytechnic University, China. His research interests include wireless/mobile communication systems, the Internet of Things, and deep learning.



JUN XING was born in 1972. He received the B.Sc. and M.Sc. degrees in computer technology and application from Northeastern University, in 1996 and 1999, respectively, and the Ph.D. degree in computer technology and application from the Dalian University of Technology, in 2008. He is currently a Lecturer with the School of Information Science and Engineering, Dalian Polytechnic University, China. His research interests include the Internet of Things and large data algorithms.

...